Desalination and Water Treatment
www.deswater.com
1944-3994 / 1944-3986 © 2011 Desalination Publications. All rights reserved.
doi: 10.5004/dwt.2011.2689

32 (2011) 139–144
August

Comparison of kinetic models for predicting phosphate adsorption onto spent alum sludge in a continuous fixed-bed column

Yao-Sen Chen[a], Wei-Chin Chang[b]*, Shun-Hsing Chuang[c], Shih-Min Chiang[d]

[a]*Graduate School of Engineering Science and Technology, National Yunlin University of Science and Technology, Touliu, 640, Yunlin County, Taiwan*
Tel. +886 (5) 5342601 ext.4495; Fax +886 (5) 5312069; email: g9314206@yuntech.edu.tw
[b]*Department of Safety, Health and Environmental Engineering, National Yunlin University of Science and Technology, Touliu, 640, Yunlin County, Taiwan*
Tel. +886 (5) 5342601 ext.4422; Fax +886 (5) 5312069; email: changwc@yuntech.edu.tw
[c]*Department of Environmental Engineering and Management, Chaoyang University of Technology, Taichung County, Taiwan*
Tel. +886 (4) 23323000 ext.4447; Fax: +886 (4) 23742365; email: shchuang@mail.cyut.edu.tw
[d]*Bureau of Environmental Protection of Tainan County, Hsing-Ying, 730, Taiwan*
Tel. +886 (6) 6572916; Fax +886 (6) 6564105; email: smchiang@mail.tnceep.gov.tw

Received 1 August 2010; Accepted in revised form 22 December 2010

ABSTRACT

This study attempted to examine the effectiveness of fixed bed adsorption for phosphate removal by spent alum sludge. Experiments with different bed depths were conducted to evaluate their effects on the column performance, where different breakthrough curves were obtained and thereby compared by kinetic models. Experimental data confirmed that expanding bed height could apparently increase the equilibrium phosphate uptake and hence lengthen both the breakthrough time and exhausting time. Spent alum sludge was concluded in this study to be successfully employed in fixed bed column for removing phosphate from aqueous solution. Furthermore, five kinetic models (Adams–Bohart, Thomas, Clark, Yoon–Nelson and bed-depth/service time analysis (BDST) models) were applied to experimental data to predict the breakthrough behavior and to determine the characteristic parameters of the column that are valuable for process design. Result indicated that both Thomas and Yoon–Nelson models described appropriately the whole breakthrough curves; whereas, BDST and Adams–Bohart models were merely suitable for fitting the initial stage of the same curves. Clark model, nevertheless, could not fit well with the experimental data.

Keywords: Breakthrough curve; Fixed-bed column; Phosphate adsorption; Alum sludge; Kinetic model

1. Introduction

Phosphate enrichment can stimulate algae blooms, degrade water quality and eventually lead to eutrophication in lakes. Reducing the phosphate concentration in incoming wastewater to meet the effluent standards was consequently inevitable for preventing an eutrophication problem in receiving water bodies. During past decades, various techniques, including physical method, biological treatment and chemical precipitation/adsorption, have been commonly suggested to be effective for removing phosphate from aqueous solution.

* Corresponding author.

Presented at the Third International Conference on Challenges in Environmental Science & Engineering, CESE-2010 26 September – 1 October 2010, The Sebel, Cairns, Queensland, Australia

Recently, a variety of low cost and easily available materials, like synthesized goethite, commercial alumina, commercial hydrotalcite [1], activated alumina [2], fly ash [3], iron oxide tailing [4] and lithium intercalated gibbsite [5], were extensively investigated. These recycled materials were recognized from these studies as successful adsorbents to remove phosphate, implying that they were potential alternatives to the conventional precipitation method. Although the spent alum sludge has also been previously verified to be capable of adsorbing phosphate from wastewater, most of the reported studies were conducted in batch modes so as to explore the adsorption capacity of sludge [6], the characteristics and mechanisms of adsorption [7], the effectiveness of sludge in removing different phosphorus species [8] and influence of sludge aging on phosphate adsorption [9]. Furthermore, only few studies have been reported on the application of alum sludge to the phosphate adsorption in a continuous fixed bed column.

This study, therefore, attempted to examine the effectiveness of fixed bed adsorption for phosphate removal by alum sludge. The experimental data obtained were further applied to five kinetic models (Adams–Bohart, Thomas, Clark, Yoon–Nelson and bed-depth service time (BDST)) so as to compare their prediction behavior. The average percentage errors between the experimental and predicted values were calculated to evaluate the adequacy of the above model equations.

2. Materials and methods

2.1. Materials

The spent alum sludge used in this study was obtained from the sedimentation tank of Feng-Yuan Water Purification Plant, Taichung City, Taiwan. The sampled sludge was freezing-dried, grounded and then stored in the dried cabinet for further experiments.

2.2. Preparation of PO_4^{3-} solutions

A stock PO_4^{3-} solution (1000 mg/L) was prepared in distilled water using potassium dihydrogen phosphate (KH_2PO_4). All experimental solutions of PO_4^{3-} were prepared by diluting this stock solution to approximately 4.7 mg P/L. The initial pH of experimental solution was between 6.5 and 6.8.

2.3. Column experiments

The schematic diagram of the fixed bed column experiment is shown in Fig. 1. Three fixed bed columns were vertically constructed in series. The fixed-bed columns were made of Perspex tubes with 3 cm internal diameter and 30 cm in height. Each column used in the experiments was packed with 10 cm alum sludge. The filter membrane and glass beads were placed at the top and bottom of the sludge to prevent any loss of sludge. The influent feed was pumped upward through the column at a constant flow rate of 6 mL/min. The effluent solutions sampled from each column were analyzed by using spectrophotometer to determine their phosphate concentrations. The column experiments were continued until a constant concentration of effluent PO_4^{3-} was obtained.

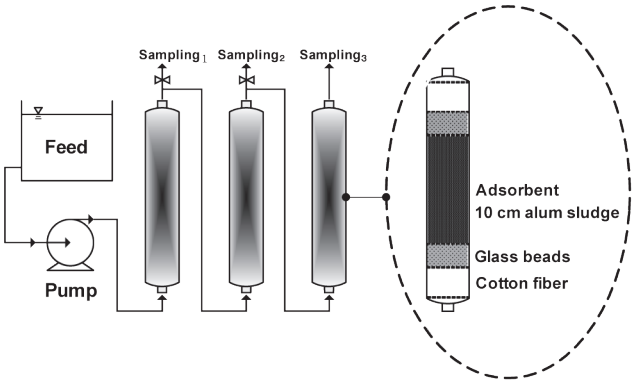

Fig. 1. The schematic diagram of a continuous fixed bed column experiment.

3. Results and discussion

3.1. Column adsorption

The breakthrough curves for phosphate adsorption onto alum sludge at different bed depths (10, 20, and 30 cm) are depicted in Fig. 2, by plotting C/C_0 (the ratio of effluent and influent phosphate concentration) vs. time (t). The resulting curves shown in Fig. 2 followed the typical S-shape profile of column adsorption. When bed depth expanded, the breakthrough curves shifted from left to right and the slope of curves tilted downward gradually, implying that more PO_4^{3-} ions were removed. Additionally, the breakthrough time occurred later when bed depth increased.

The parameters, including breakthrough time (t_b; min), exhaust time (t_{tot}; min), total PO_4^{3-} adsorbed (q_{tot}; mg) and total PO_4^{3-} percent removal (%), were calculated by applying the adsorption data to the mathematical analysis reported in Kundu and Gupta's study [10]. The computed values of the above mentioned parameters are summarized in Table 1. Increasing bed height provided more time for phosphate to contact with the alum sludge and offered more available binding sites for adsorption. The breakthrough time, exhaustion time, equilibrium phosphate adsorption capacity and removal efficiency hence increased with the expansion in bed height, as shown in Table 1.

3.2. Estimation of breakthrough curves

To predict and analyze the dynamic behavior of phos-

Table 1
Fixed bed adsorption data at different bed depths

[a]Parameter	Breakthrough time t_b (min)	Exhausting time t_{tot} (min)	Total PO_4^{3-} sorbed q_{tot} (mg)	Total PO_4^{3-} removal (%)
[b]Bed depth, h (cm)				
10 (m = 43.4 g)	10	130	1.56	42.5
20 (m= 86.8 g)	70	210	3.32	56.0
30 (m= 130.2 g)	130	290	5.11	62.5

[a]Breakthrough concentration $C_b = 0.1C_0$; Exhausting concentration $C_e = 0.8C_0$
Total adsorbed PO_4^{3-} quantity (mg), $q_{tot} = 1/1000 \int_{t=0}^{t=tot} C_{ads}dt$, $C_{ads} = C_0 - C$
Total PO_4^{3-} removal (%) = $(q_{tot}/X) \times 100$
Total amount of PO_4^{3-} (mg), $X = C_0Qt_{tot}/1000$
[b]C_0 = 4.7 mg/L, Q = 6 mL/min

phate adsorption onto alum sludge in a fixed-bed column, five kinetic models, including Adams–Bohart, Thomas, Yoon–Nelson, BDST and Clark models, were applied to the experimental data. The average percentage errors (ε%), indicating the differences between the experimental and predicted values of C/C_0, were calculated by the following equation suggested by [11]:

$$\varepsilon\% = \frac{\sum_{i=1}^{N}\left|\left(\left(C/C_0\right)_{\exp} - \left(C/C_0\right)_{theo}\right)/\left(C/C_0\right)_{\exp}\right|}{N} \times 100 \quad (1)$$

where N is the number of measurements.

3.3. Application of the Adams–Bohart model

The Adam–Bohart model, which is the most established model and is commonly used to describe of the initial stage of the breakthrough curve, is listed as follows [11–13]:

$$\ln\frac{C}{C_0} = k_{AB}C_0t - k_{AB}N_0\frac{Z}{U_0} \quad (2)$$

where C_0 and C are the inlet and effluent phosphate concentrations (mg/L), respectively. k_{AB} is the kinetic constant (L/mg min), U_0 is the linear velocity calculated by dividing the flow rate by the column section area (cm/min), Z is the bed depth of column (cm) and N_0 is the saturation concentration (mg/L). According to this equation, the operational parameters of the column, i.e. k_{AB} and N_0, can be determined from a plot of lnC/C_0 against t at a given bed height and flow rate.

Fig. 2 compares the experimental and predicted breakthrough curves for phosphate adsorption onto alum sludge at different bed depths by applying Adams–Bohart model to the varying data regions (the ratios of C/C_0 from zero to 0.15, 0.4, 0.6 and 0.8, respectively). Excellent fitting results were apparently achieved during the initial stage of every breakthrough curve illustrated in Fig. 2. Similar studies, i.e., biosorption of phenol by immobilized activated sludge [11] and adsorption of congo red by use of rice husk [12], reported that the model was valid in C/C_0 from zero up to 0.5. Fig. 2 reveals that superior agreement with the initial part of the data was attained in the C/C_0 region from zero to 0.4 or 0.6, suggesting that the model's validity for the relative concentration region of C/C_0 could be up to 0.6. Conversely, comparatively larger discrepancies were found between the experimental data and predicted curves while the range of modeled data was as low as 0.15 or high as 0.8. These findings implied that the Adams–Bohart model was valuable for the initial part of breakthrough curves from phosphate adsorption on alum sludge in columns. Table 2 presents the values of k_{AB} and N_0 at different bed depths by applying the model to data region from zero to 0.6. The values of kinetic constant and saturation concentration decreased with the increase of the bed depth.

3.4. Application of the Thomas model

The Thomas model was developed to calculate the maximum solid phase concentration of solute on the sorbent and the adsorption rate constant for an adsorption column. Traditionally, this model is used to design the maximum adsorption capacity of an adsorbent. The model is given as follows [11–13]:

$$\ln\left(\frac{C_0}{C} - 1\right) = \frac{k_{Th}q_0m}{Q} - \frac{k_{Th}C_0V_{eff}}{Q} \quad (3)$$

where k_{Th} is the Thomas rate constant (mL/mg min), q_0 the equilibrium PO_4^{3-} uptake per gram of the adsorbent (mg/g) and m is the amount of adsorbent in the column (g). The kinetic coefficient k_{Th} and the adsorption capacity of the column q_0 can be determined from a plot of $\ln((C_0/C) - 1)$ against t (= V_{eff}/Q) at a given flow rate.

Fig. 3 shows the experimental data and predicted breakthrough curves obtained from the Thomas model. The values of k_{Th} and q_0 obtained by using Eq. (3) are presented in Table 3. As can be seen from Fig. 3, the effluent

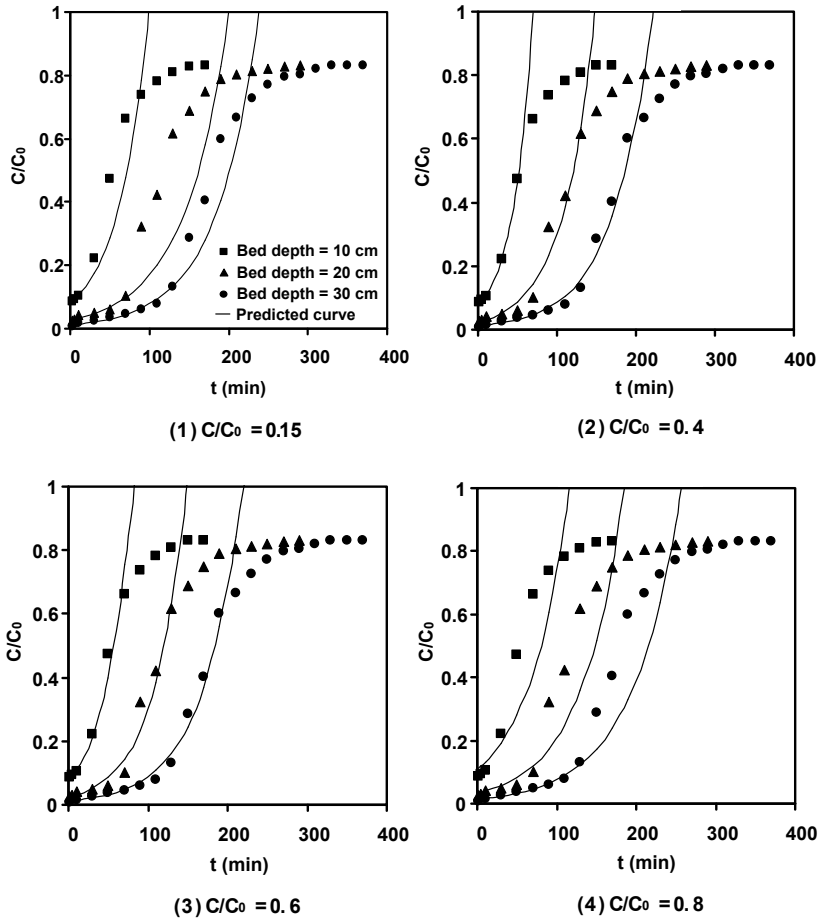

Fig. 2. Comparison of experimental and predicted breakthrough curves for phosphate adsorption onto alum sludge by applying Adams–Bohart model to the varying data regions (the ratios of C/C_0 from zero to 0.15, 0.4, 0.6 and 0.8, respectively).

Table 2
Parameters of Adams–Bohart model by applying the data region (C/C_0) from zero to 0.6

Z (cm)	k_{AB} (L/mg min)	N_0 (mg/L)	R^2
30	0.0044	29.1	0.981
20	0.0053	29.7	0.963
10	0.0068	31.4	0.987

Table 3
Parameters of the Thomas model at different bed depths

Z (cm)	k_{Th} (mL/mg min)	q_0 (mg/g)	R^2	ε (%)
30	4.81	0.0430	0.977	17.13
20	5.72	0.0435	0.963	18.59
10	6.98	0.0441	0.942	14.77

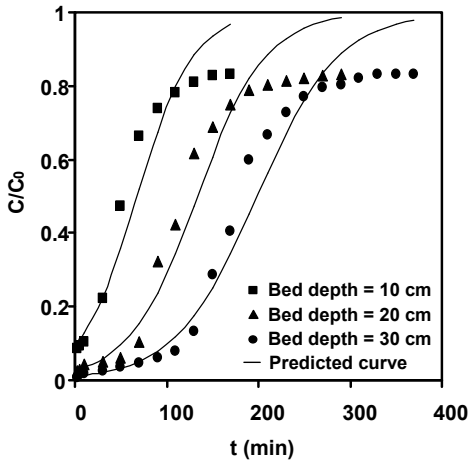

Fig. 3. Comparison of experimental data and predicted breakthrough curves by using the Thomas model.

concentration predicted by the model was apparently compatible with the experimental data. Besides, from

the average percentage errors (<18.59 %) and R^2 values in Table 3, an acceptable differences was observed between the experimental and predicted values. This result suggested that the model was suitable for describing the whole breakthrough curves and could be properly used in predicting the exhaustion time.

3.5. Application of the Yoon–Nelson model

The Yoon and Nelson model is based on the assumption that the rate of decrease in the probability of adsorption for each adsorbate molecule is proportional to the probability of adsorbate adsorption and the probability of adsorbate breakthrough on the adsorbent. This model is less complicated than other models. The equation regarding to a single component system is expressed as follows [11–13]:

$$\ln\frac{C}{C_0 - C} = k_{YN}t - \tau k_{YN} \quad (4)$$

where k_{YN} is the rate constant (1/min) and τ is the time required for 50% adsorbate breakthrough (min). The values of the model parameters k_{YN} and τ can be determined from the slope and intercept of the linear plot of $\ln(C/(C_0 - C))$ vs. sampling time (t) according to Eq. (4).

The theoretical breakthrough curves predicted by the Yoon–Nelson model, together with the corresponding experimental data, are shown in Fig. 4. This figure obviously exhibits that the Yoon–Nelson model fitted appropriately the experimental data (C/C_0) ranging from zero up to 0.8. That is, the model provided good description of almost the whole breakthrough curves and could suitably predict the exhaustion time of the adsorption behavior. Additionally, the values of k_{YN} and τ with respect to various bed depths are listed in Table 4. This table confirms a negligible difference between the experimental and the calculated τ values, indicating that the Yoon–Nelson model was suitably applied to the alum sludge adsorption processes.

3.6. Application of the BDST model

The BDST model describes a relationship between the service time and the packed-bed depth of the column. The BDST model has been widely used for predicting breakthrough curves and designing columns. The model is represented as follows [12,14]:

$$t = \frac{N_0}{C_0 U_0}Z - \frac{1}{k_B C_0}\ln\left(\frac{C_0}{C} - 1\right) \quad (5)$$

where k_B is the adsorption rate constant (L/mg min) and t is the service time to breakthrough (min). Experimental data are used to estimate the characteristic parameters, k_B and N_0, from the slope and intercept of Eq. (5).

Fig. 5 depicts the breakthrough curves predicted from the BDST model. The respective values of k_B and N_0 at different bed depths are presented in Table 5. As is shown in Fig. 5, fine fitting was only obtained in the initial region of the breakthrough curves. Significant discrepancies obviously exists between the BDST predicted values and experimental data above break points ($C = 0.1C_0$). The BDST model hence was implied by the above results to perform poorly in predicting the whole breakthrough curves.

Table 4
Parameters of the Yoon–Nelson model at different bed depths

Z (cm)	k_{YN} (1/min)	τ_{theo} (min)	τ_{exp} (min)	R^2	ε (%)
30	0.0240	191.7	190	0.967	17.54
20	0.0293	127.7	110	0.932	18.21
10	0.0469	54.1	50	0.990	11.48

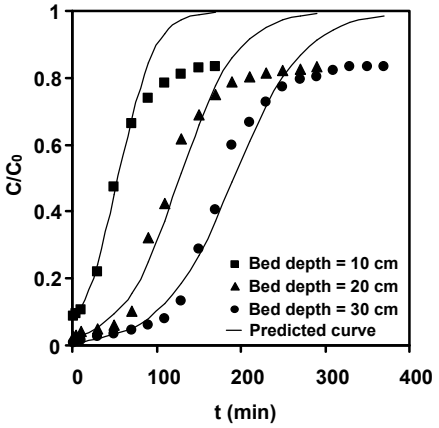

Fig. 4. Comparison of experimental data and predicted breakthrough curves by using the Yoon–Nelson model.

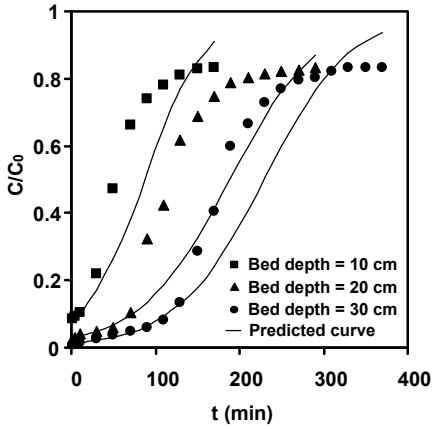

Fig. 5. Comparison of experimental and predicted breakthrough curves by using the BDST model.

Table 5
Parameters of the BDST model at different bed depths

Z (cm)	k_a (L/mg min)	N_0 (mg/L)	R^2	ε (%)
30	0.0041	30.5	0.961	18.44
20	0.0040	37.7	0.934	24.62
10	0.0059	34.7	0.993	15.82

3.7. Application of the Clark model

The Clark model associates the Freundlich equation and the mass transfer concept to define a new simulation of breakthrough curves. The mathematical equations for Clark model is listed as follows [11,15]:

$$\ln\frac{C}{C_0}=\frac{1}{\left(1+Ae^{-\theta * t}\right)^{1/n-1}} \tag{6}$$

$$A=\left(\frac{C_0^{n-1}}{C_b^{n-1}}-1\right)e^{\theta * t_b} \tag{7}$$

$$\theta=\frac{k_{Cl}}{U_0}\nu(n-1) \tag{8}$$

$$\nu=\frac{U_0C_0}{N_0+C_0} \tag{9}$$

where k_{Cl} and n are the mass transfer coefficient (1/min) and the Freundlich constant. t_b and C_b are the time and outlet concentration at breakthrough point, respectively. Eqs. (7)–(9) can be utilized by non-linear regression to determine the values of A and θ. The breakthrough curve can be predicted according to the relationship between C/C_0 and t in Eq. (6).

The breakthrough curves predicted by the Clark model are plotted in Fig. 6 by supposing the Freundlich constant in Eq. (6) vary from 2 to 6. Besides, the coefficient k_{Cl} (1/min) was assumed to be the same as k_{YN} (1/min) calculated from the Yoon–Nelson model. Fig. 6 obviously shows that the whole breakthrough curves simulated by Clark model could not fit well with experimental data. Enlarging the n values from 2 to 6 clearly shifted the curves from left to right, showing extremely poor agreement between the experimental and predicted values. Theses results clarified that the Clark model was improper to be applied to phosphate adsorption onto alum sludge.

4. Conclusions

a) The spent alum sludge, as an adsorbent in a continuous fixed bed column, was capable of removing phosphate from aqueous solution. Expanding bed height could apparently increase the equilibrium phosphate uptake and thus lengthen the breakthrough time and exhaustion time.
b) The Adams–Bohart model fitted suitably the initial region of breakthrough curves and predicted adequately the breakthrough time. Particularly, the model's validity for the relative concentration region of C/C_0 could be extended up to 0.6.
c) The Thomas and Yoon–Nelson models described suitably the whole breakthrough curves and predicted properly both the breakthrough and exhaustion time; whereas, the BDST model fitted well for merely a limited portion of adsorption behavior.
d) The Clark model clearly could not simulate well the phosphate adsorption behavior of spent alum sludge in fixed bed column.

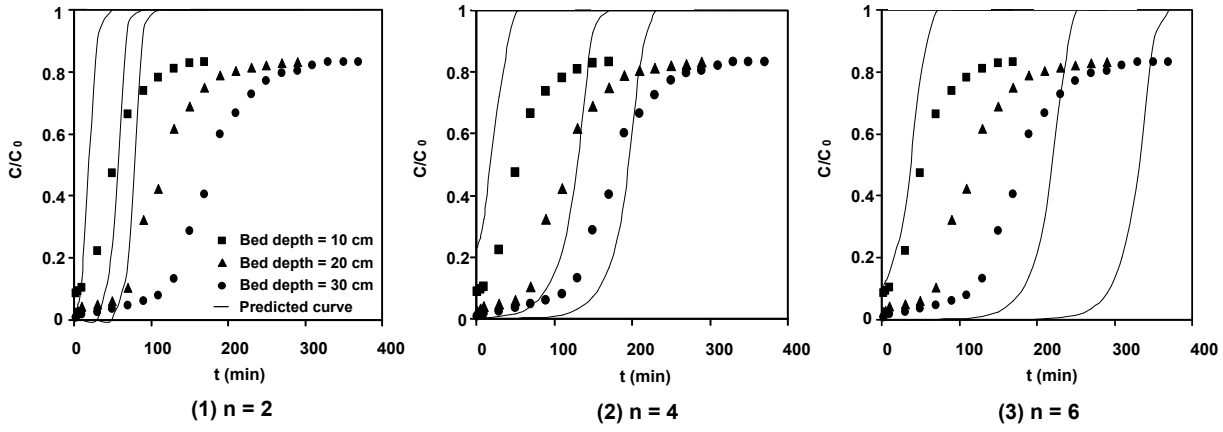

Fig. 6. Comparison of experimental data and predicted breakthrough curves by using the Clark model and assuming various Freundlich constant (n) values.

Acknowledgement

The authors would like to thank the CECI Engineering Consultants, Inc., for financially supporting this research under Contract No. 94927.

References

[1] E.N. Peleka and E.A. Delyannis, Adsorptive removal of phosphate from aqueous solutions, Desalination, 245 (2009) 357–371.
[2] T. Hano, H. Takanashi, M. Hirata and K. Urano, Removal of phosphorus from wastewater by activated alumina adsorbent, Wat. Sci. Technol., 35 (1997) 39–46.
[3] K.C. Cheung and T.H. Venkitachalam, Improving phosphate removal of sand infiltration system using alkaline fly ash, Chemosphere, 41 (2000) 243–249.
[4] L. Zeng, X. Li and J. Liu, Adsorptive removal of phosphate from aqueous solutions using iron oxide tailings, Wat. Res., 38 (2004) 1318–1326.
[5] S.L. Wang, C.Y. Cheng, Y.M. Tzou, R.B. Liaw, T.W. Chang and J.H. Chen, Phosphate removal from water using lithium intercalated gibbsite, J. Hazard. Mater., 147 (2007) 205–212.
[6] S.H. Huang and B. Chiswell, Phosphate removal from wastewater using spent alum sludge, Wat. Sci. Technol., 42 (2000) 295–300.
[7] Y. Yang, Y.Q. Zhao, A.O. Babatunde, L. Wang, Y.X. Ren, and Y. Han, Characteristics and mechanisms of phosphate adsorption on dewatered alum sludge, Separ. Purif. Technol., 51 (2006) 193–200.
[8] M. Razali, Y.Q. Zhao and M. Bruen, Effectiveness of a drinking-water treatment sludge in removing different phosphorus species from aqueous solution, Separ. Purif. Technol., 55 (2007) 300–306.
[9] Y. Yang, Y.Q. Zhao and P. Kearney, Influence of ageing on the structure and phosphate adsorption capacity of dewatered alum sludge, Chem. Eng. J., 145 (2006) 276–284.
[10] S. Kundu and A.K. Gupta, As(III) removal from aqueous medium in fixed bed using iron oxide-coated cement (IOCC): Experimental and modeling studies, Chem. Eng. J., 129 (2007) 123–131.
[11] Z. Aksu and F. Gonen, Biosorption of phenol by immobilized activated sludge in a continuous packed bed: Prediction of breakthrough curve, Process Biochem., 39 (2004) 599–613.
[12] R. Han, D. Ding, Y. Xu, W. Zou, Y. Wang, Y. Li and L. Zou, Use of rice husk for the adsorption of congo red from aqueous solution in column mode, Bioresour. Technol., 99 (2008) 2938–2946.
[13] E. Malkoc, Y. Nuhoglu, and Y. Abali, Cr(VI) adsorption by waste acorn of quercus ithaburensis in fixed beds: Prediction of breakthrough curves, Chem. Eng. J., 119 (2006) 61–68.
[14] T.S. Singh and K.K. Pant, Experimental and modelling studies on fixed bed adsorption of As(III) ions from aqueous solution, Separ. Purif. Technol., 48 (2006) 288–296.
[15] Y. Sag and Y. Aktay, Application of equilibrium and mass transfer models to dynamic removal of Cr(VI) ions by chitin in packed column reactor, Process Biochem., 36 (2001) 1187–1197.